Adv. Composite Mater., Vol. 16, No. 1, pp. 1–10 (2007)

Also available online - www.brill.nl/acm

Electrical properties of ABS resin reinforced with recycled CFRP

TAKASHI NISHIKAWA [1], KEIJI OGI [1,*], TOSHIRO TANAKA [1], YASUTAKA OKANO [2] and ICHIRO TAKETA [3]

[1] *Department of Materials Science and Engineering, Ehime University, 3, Bunkyocho, Matsuyama, Ehime 790-8577, Japan*
[2] *Panasonic Shikoku Electronics Co., Ltd., 247, Fukutake, Saijo, Ehime 793-8510, Japan*
[3] *Toray Industries, Inc., 1515, Tsutsui, Masaki-cho, Ehime 791-3193, Japan*

Received 3 October 2005; accepted 14 December 2005

Abstract—Composite materials consisting of crushed carbon fiber reinforced plastics (CFRP) pieces and acrylonitrile-butadiene-styrene (ABS) resin were prepared by an injection mold method to solve the problem of recycling of CFRP. The electrical properties, such as electrical resistivity, alternating current impedance and electromagnetic interference (EMI) shielding effect, were measured for the composites. The electrical resistivity of the composites showed a percolation type of conduction behavior and no difference between parallel and perpendicular to the injection direction was observed for CFRP content higher than the critical value. Measurement of alternating current impedance revealed that the conduction mechanism is attributed to the direct conductive paths generated by distributed carbon fibers; however, strong frequency dependence of the impedance was observed for the CFRP content near the critical one. The frequency dependence of the impedance is caused by the inter-fiber connection and can be expressed as a simple equivalent circuit. The absorption component of shielding effect (SE) was smaller than the expected value estimated from its resistivity. The decline of SE is thought to be caused by the decrease in effective thickness due to fiber orientation.

Keywords: CFRP; recycle; alternating current impedance; EMI shielding.

1. INTRODUCTION

With the rapid development of electronics, electromagnetic interference (EMI) effects have attracted much attention because they prevent normal operation of the electronic devices and are believed to be detrimental to human health [1–3]. Hence, EMI shielding materials which protect the electronic equipment and the human body from the electromagnetic radiation emanating from electronic devices have been developed energetically.

*To whom correspondence should be addressed. E-mail: kogi@eng.ehime-u.ac.jp

Carbon fiber reinforced plastics (CFRP) have been widely used for many purposes because of their excellent mechanical properties. As a carbon fiber (CF) is an electrical conductor, the CFRP also has a conducting nature and will be applicable to electromagnetic interference (EMI) shield materials [4]. As the use of CFRP products has become more widespread, the problem of their recycling has arisen: the recycling of CFRP is thought to be difficult because of its strength and chemical stability.

In order to develop the recycling of CFRP wastes, composite materials were fabricated by mixing crushed CFRP pieces with acrylonitrile-butadiene-styrene (ABS) resin. The mechanical properties of the composite materials have been reported elsewhere [5]. As the crushed CFRP pieces act as conducting filler, the composite material is an electrical conductor and expected to have an EMI shielding effect.

In this paper, the electrical resistivity, alternating current impedance and EMI shielding effect were measured to investigate the electrical properties of the above composite materials with various CFRP contents. Firstly, the dependence of CFRP content on the electrical resistivity is discussed based on the percolation theory. Secondly, the impedance behavior is explained with the use of an equivalent electrical circuit. Finally, the EMI shielding effect is evaluated as a complex effect of the reflection and absorption mechanisms.

2. EXPERIMENTAL

The composite materials used in the present study consisted of recycled CFRP pieces and ABS resin. The recycled CFRP was polyacrylonitrile (PAN)-based CF and epoxy resin having a multidirectional laminate structure; the CF volume fraction V_f is about 60%. The CFRP pieces with an average size of 3.40 mm × 0.40 mm × 0.05 mm were made by crushing CFRP wastes. Square plates (150 mm × 150 mm × 3 mm) were formed for various CFRP contents by an injection mold method. The weight and volume fraction of CFRP together with the calculated volume fraction of CF are shown in Table 1.

Alternating current impedance was measured by a four-terminal method by using an LCR meter (Agilent 4284A). The impedance was measured at a frequency ranging from 1 kHz to 1 MHz and the DC resistivity was estimated from the data at a low frequency.

Table 1.
Weight and volume fraction of CFRP and volume fraction of CF in CFRP/ABS composites

Sample number	0 (ABS)	1	2	3	4	5	6	7	8 (CFRP)
CFRP content (wt.%)	0	10	20	30	40	50	60	70	100
CFRP content (vol.%)	0.0	6.8	14.1	22.0	30.4	39.6	49.6	60.5	100.0
CF content (vol.%)	0.0	4.1	8.5	13.2	18.2	23.8	29.8	36.4	60.0

EMI shielding effect on the basis of the Advantest method was measured at a frequency varying between 60 MHz and 1.2 GHz with the aid of a network analyzer (HP 8720C). Shielding effectiveness *SE* was defined as:

$$SE = -\log_{10}\left(\frac{E_1}{E_0}\right), \tag{1}$$

where E_1 and E_0 denote the electric fields in the presence and absence of the shield, respectively.

Because the electrical properties measured in the present work are bulk or macroscopic ones, their variation among samples with the same CFRP content is negligible. Therefore, electrical measurements were carried out using one or two samples for each CFRP content. Reproducibility was checked by several times of measurement.

3. RESULTS AND DISCUSSION

3.1. Conducting behavior

Electrical resistivity of the samples measured in parallel and vertical to the injection direction was plotted against CFRP content in Fig. 1. Both samples with intermediate CFRP content showed almost the same resistivity values. Therefore, the conductivity of the composite samples is considered to be insensible to the direction of the in-plane applied current. The in-plane electrical isotropy is thought to be attributed to the fiber orientation [5]. Most carbon fibers are randomly distributed

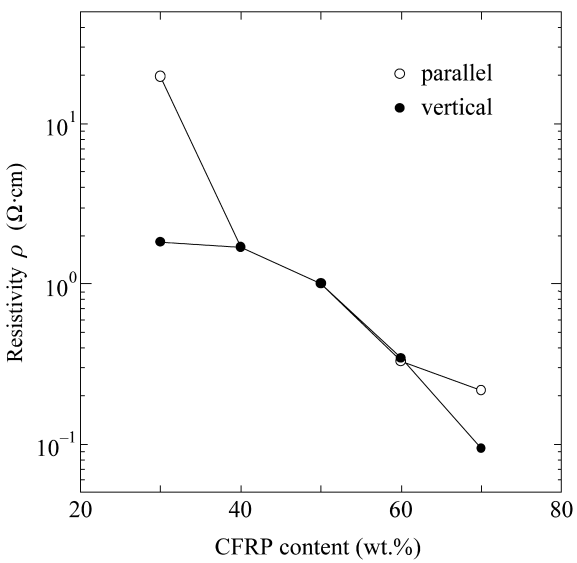

Figure 1. Electrical resistivity ρ plotted against CFRP content. Open and closed circles denote ρ values measured in parallel and vertical to the injection direction, respectively.

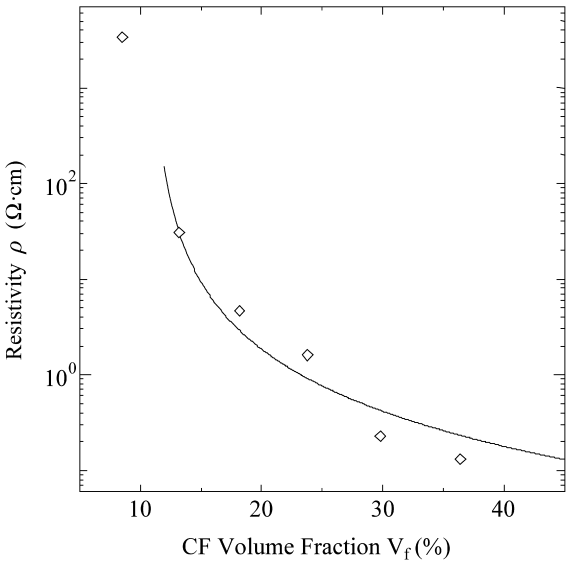

Figure 2. Electrical resistivity plotted against CF volume fraction. Solid line denotes a fitting curve using equation (3).

in the ABS resin while some fibers are oriented along the injection direction near the surface. Because of this isotropy, the data measured only in a direction parallel to the injection are discussed hereafter.

Figure 2 shows the electrical resistivity measured in the parallel direction plotted against volume fraction of CF, V_f. In general, resistivity ρ of a composite material composed of insulating matrix and conducting fillers is characterized by the volume fraction of fillers V_f and obeys the following scaling law: [6]

$$\rho = \rho_0 (V_f - V_c)^t, \tag{2}$$

where ρ_0 and t are material constant and a critical exponent, respectively, and V_c denotes a critical volume fraction which characterizes percolation behavior. The critical volume fraction V_c was reported to be inversely proportional to a square of the aspect ratio [7] and the critical exponent t was calculated to be about -2 [8]. Therefore, equation (2) is rewritten as:

$$\rho = \rho_0 \left\{ V_f - \alpha \left(\frac{D}{L} \right)^2 \right\}^{-2}, \tag{3}$$

where L and D denote a length and diameter of the filler, respectively, and α is a material constant. Fitting results for equation (3) are also shown by the solid line in Fig. 2, where ρ_0, α and V_c are calculated to be 0.015 Ω cm, 90 and 0.11, respectively, using $D = 7$ μm and $L = 200$ μm. For $V_f < V_c$, the composite shows insulating behavior, while for $V_f > V_c$, it shows conducting behavior due to involved carbon fibers which form conducting paths.

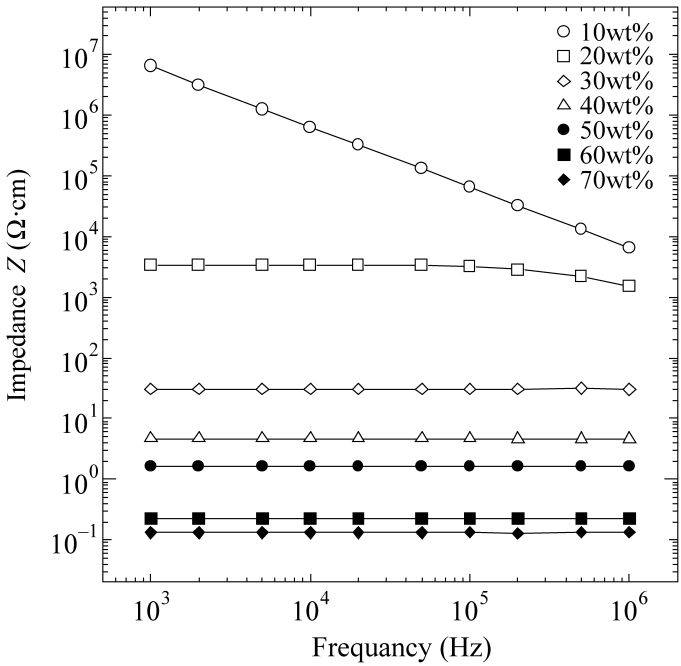

Figure 3. Frequency dependence of the alternating current impedance for various CFRP contents.

Figure 3 shows the frequency dependence of the alternating current impedance. Obvious difference of the frequency dependence between low and high CFRP content was observed. At CFRP content higher than 30 wt% ($V_f \geqslant 0.132$), the impedance does not show any frequency dependence; on the other hand, the impedance values of 10 wt% ($V_f = 0.041$) and 20 wt% ($V_f = 0.085$) samples decreases with increasing frequency. The frequency dependence of phase angle θ is shown in Fig. 4. The values of phase angle θ for 60 wt% ($V_f = 0.298$) and 10 wt% samples are respectively about 0 and -90 degrees independent of frequency. These results indicate that the impedance of the 60 wt% sample consists of only a resistance component; in contrast, the impedance for the 10 wt% sample consists of only a capacitance component. In other words, the former sample acts as a pure resistor and the latter acts as an insulator or a dielectric material. This impedance behavior is consistent with the fact that the critical volume fraction V_c is 0.11. The phase angle of the 20 wt% sample shows strong frequency dependence, indicating that the impedance involves both real and imaginary parts. The imaginary part of the impedance Z'' of 20 wt% sample is plotted against the real part Z' (Cole-Cole plot) [9] in Fig. 5. The plots are well fitted by a semicircle. This result indicates that the electrical conducting system of the present material with intermediate CFRP content is expressed as a parallel circuit of a resistance and a capacitance shown in the inset figure. The capacitance component is considered to be generated at the contact point of carbon fibers. At a CFRP content much lower than V_c, fibers are individually dispersed and do not contact with each other. Then, the material

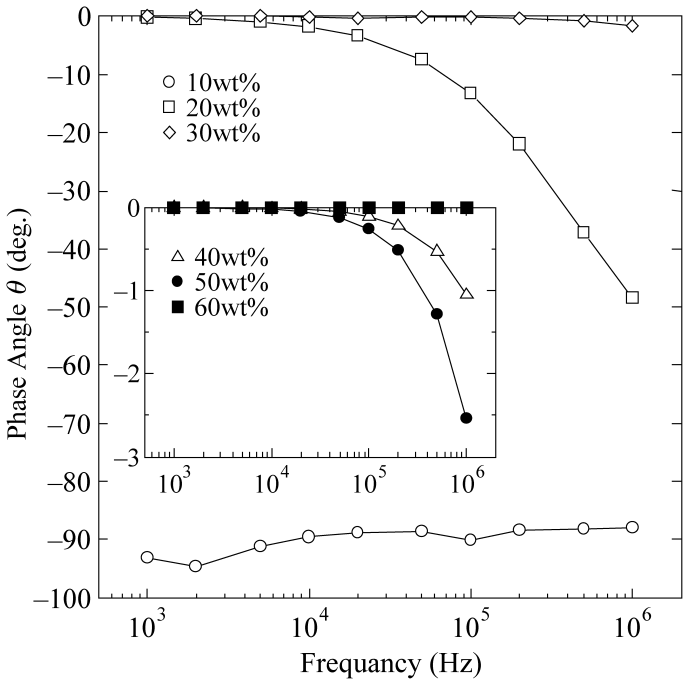

Figure 4. Frequency dependence of the phase angle θ. The inset figure shows θ for higher content samples.

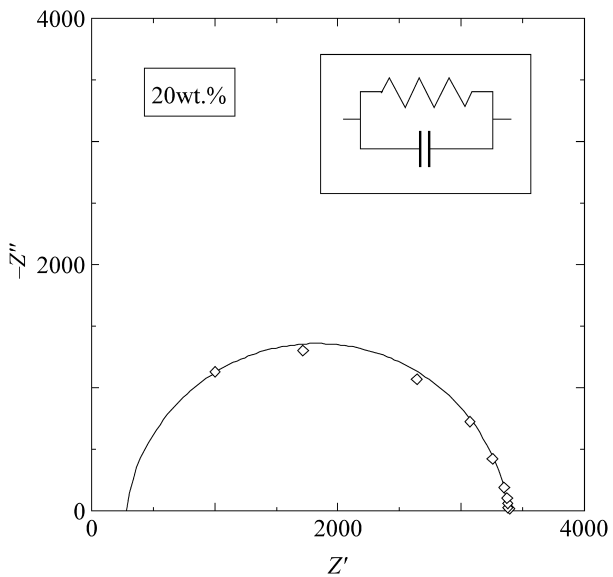

Figure 5. Imaginary part of the complex impedance of 20 wt% sample plotted against the real part (Cole–Cole plot). The inset figure shows a schematic diagram of the equivalent circuit of the composite.

behaves as a capacitor or an insulator. In contrast, at a CFRP content much higher than V_c, good connection between fibers generates conductive paths and makes the material a pure resistor. When the CFRP content is near V_c, both dielectric and conductive natures coexist in the sample, resulting in strong frequency dependence.

3.2. EMI shielding effect

Figure 6 shows the EMI shielding effect *SE* of various samples for frequency up to 1.2 GHz. The shielding effects of a pure aluminum plate and a virgin CFRP plate are also plotted for comparison. As shown in Fig. 6, *SE* increases with increasing CFRP content and reaches about −35 dB at 70 wt%. The EMI shielding effect is known to be caused by three mechanisms: reflection, absorption and multiple reflection [4]. A schematic diagram of the EMI shielding mechanisms is shown in Fig. 7. The primary contribution for EMI shielding is reflection. This mechanism requires existence of mobile carriers in the system, which interacts with the electromagnetic radiation. The second contribution, absorption, requires the electronic dipole in order to interact with the electromagnetic field. The third contribution, multiple reflection, requires a large surface area or a porous structure. If the multiple reflection is ignored, the EMI shielding effect of a conductive composite material

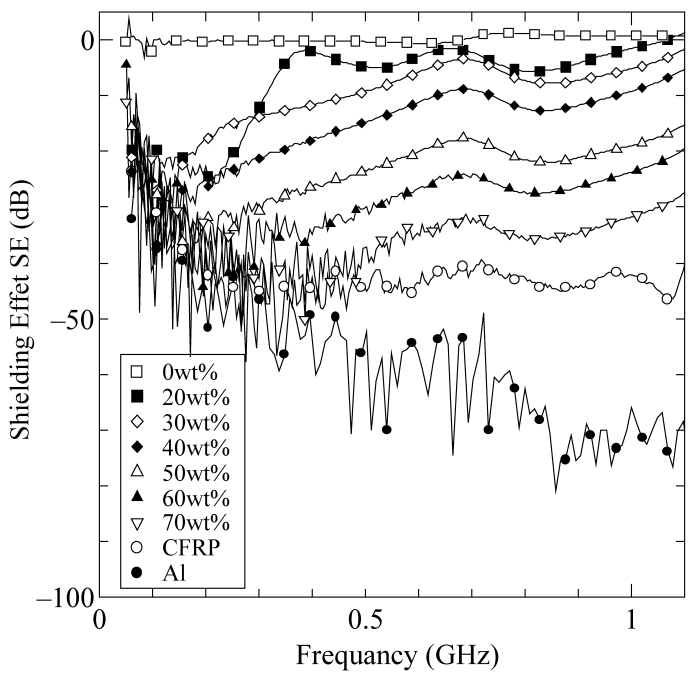

Figure 6. Frequency dependence of the EMI shielding effect *SE* plotted for various CFRP contents. *SE* of a virgin CFRP and an aluminum plates is also plotted for comparison.

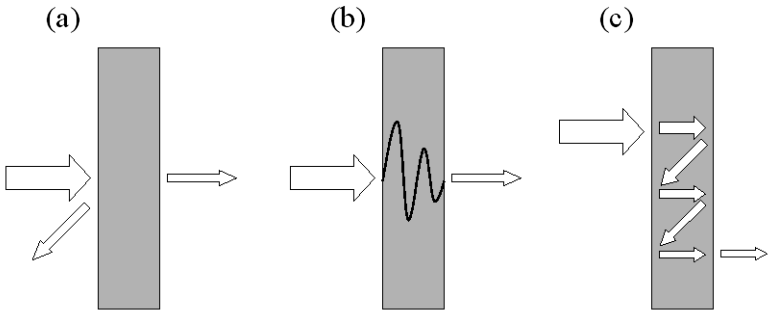

Figure 7. Schematic diagram of the EMI shielding mechanisms: (a) reflection; (b) absorption; (c) multiple reflection.

can be described by Simon formalism [10]:

$$|SE| = 50 + 10 \log \frac{1}{\rho f} + at\sqrt{\frac{f}{\rho}}, \tag{4}$$

where a is a material constant and equals about 1.7 in general. The parameters ρ, f and t represent the resistivity (Ω cm), frequency (MHz) and thickness of a shield material, respectively. The first and second terms are attributed to the reflection mechanism and the third comes from the absorption mechanism.

Calculated results of Simon's equation and measured shielding data are co-plotted in Fig. 8. Calculated values are rather larger than the experimental data. As indicated by the equation, the *SE* due to the reflection decreases with the increase of frequency. Therefore, the deviation of the calculated value from the experimental data is considered to be caused by the absorption component, which is enhanced with increasing frequency. The absorption mechanism of the EMI shielding acts continuously while the electromagnetic wave goes back and forth through the material several times. In contrast, the reflection mechanism acts only at the material's surface. Therefore, the reflection and absorption mechanisms are considered to be associated with the surface resistance and the out-of-plane resistance, respectively. In Simon's formula, three-dimensional isotropy of resistivity is assumed; however, both mechanisms are related with in-plane and out-of-plane resistivity, which are not always the same. Hence, the material constant a is treated as a fitting parameter for practical estimation of contribution of absorption mechanism to the EMI shielding. The predictions using $a = 0.1$ give good agreement with the experimental results. This means that the contribution of the absorption component is much smaller than that of ordinary material with $a = 1.7$. The reason why the value of a is smaller than the expected value may be the high vertical resistance. Because of the large aspect ratio of fibers, fewer fibers are expected to be oriented in the out-of-plane direction than in the in-plane direction, which causes the vertical resistance to be higher than the horizontal one. This higher vertical resistance results in the effective thickness for the absorption mechanism smaller than the actual one. Consequently, the constant a associated

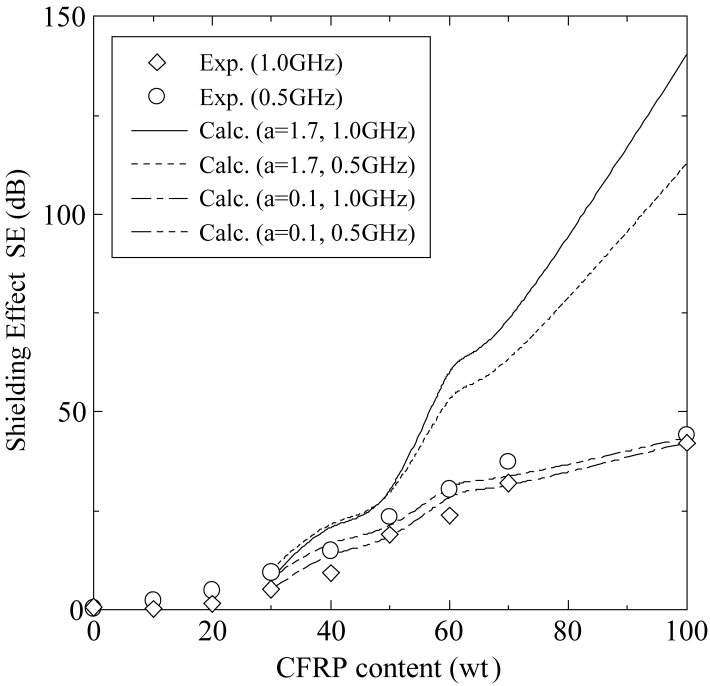

Figure 8. Comparison of *SE* between measured values and predictions using equation (4). Solid and dashed lines denote calculations using $a = 1.7$. Dot-dashed and 2-dot-dashed lines denote modified results using $\alpha = 0.1$.

with the absorption component becomes smaller than a general value, leading to the lower measured value of *SE*.

4. CONCLUSION

Electrical properties of crushed CRRP pieces/ABS resin composites were measured for various CFRP contents. The electrical resistivity decreases with increasing CFRP content and the critical volume fraction V_c is estimated to be 0.11. At volume fraction near V_c, the impedance of the sample is characterized by a simple equivalent circuit composed of both resistance and capacitance components. The absorption component of the EMI shielding effect is much smaller than the expected value due to low conductivity in the out-of-plane direction.

Acknowledgement

This study was supported by a Grant-in-Aid for Cooperation of Innovative Technology and Advanced Research In Evolutional Area (CITY AREA), 2004, from the Ministry of Education, Culture, Sports, Science and Technology of Japan.

REFERENCES

1. D. M. Bigg and D. E. Stutz, Plastic composites for electromagnetic interference applications, *Polym. Compos.* **4**, 40–46 (1983).
2. D. M. Bigg, Effect of chemical exposure on the EMI shielding of conducting plastics, *Polym. Compos.* **8**, 1–7 (1987).
3. N. C. Das, D. Khastgir, T. K. Chaki and A. Chakraborty, Electromagnetic interference shielding effectiveness of carbon black and carbon fibre filled EVA and NR based composites, *Composites Part A* **31**, 1069–1081 (2000).
4. Xi Luo and D. D. L. Chung, Electromagnetic interference shielding using continuous carbon-fiber carbon-matrix and polymer-matrix composites, *Composites Part B* **30**, 227–231 (1999).
5. K. Ogi, T. Nishikawa, Y. Okano and I. Taketa, Mechanical properties of ABS resin reinforced with recycled CFRP (submitted to *Advanced Composite Materials*).
6. D. Stauffer, *Introduction to Percolation Theory*, Taylor and Francis, Philadelphia (1985).
7. F. Carmona, F. Barreau, P. Delhaes and R. Canet, An experimental model for studying the effect of anisotropy on percolative conduction, *J. Physique Lett.* **41**, L531–L534 (1980).
8. W. Y. Hsu, W. G. Holtje and J. R. Barkley, Percolation phenomena in polymer/carbon composites, *J. Mater. Sci. Lett.* **7**, 459–462 (1988).
9. K. S. Cole and R. H. Cole, Dispersion and absorption in dielectrics, *J. Chem. Physics* **9**, 341–351 (1941).
10. R. T. Simon, EMI shielding through conductive plastics, *Polym. Plast. Technol. Eng*. **17**, 1–10 (1981).